J. Cent. South Univ. (2019) 26: 2785−2796
DOI: https://doi.org/10.1007/s11771-019-4213-5

Springer

Thermoelastic vibration analysis of micro-scale functionally graded material fluid-conveying pipes in elastic medium

TONG Guo-jun(仝国军), LIU Yong-shou(刘永寿), LIU Hui-chao(刘会超), DAI Jia-yin(戴嘉茵)

School of Mechanics, Civil Engineering and Architecture, Northwestern Polytechnical University, Xi'an 710129, China

Abstract: Micro-scale functionally graded material (FGM) pipes conveying fluid have many significant applications in engineering fields. In this work, the thermoelastic vibration of FGM fluid-conveying tubes in elastic medium is studied. Based on modified couple stress theory and Hamilton's principle, the governing equation and boundary conditions are obtained. The differential quadrature method (DQM) is applied to investigating the thermoelastic vibration of the FGM pipes. The effect of temperature variation, scale effect of the microtubule, micro-fluid effect, material properties, elastic coefficient of elastic medium and outer radius on thermoelastic vibration of the FGM pipes conveying fluid are studied. The results show that in the condition of considering the scale effect and micro-fluid of the microtubule, the critical dimensionless velocity of the system is higher than that of the system which calculated using classical macroscopic model. The results also show that the variations of temperature, material properties, elastic coefficient and outer radius have significant influences on the first-order dimensionless natural frequency.

Key words: functionally graded materials; thermoelastic vibration; micro-scale; micro-fluid

Cite this article as: TONG Guo-jun, LIU Yong-shou, LIU Hui-chao, DAI Jia-yin. Thermoelastic vibration analysis of micro-scale functionally graded material fluid-conveying pipes in elastic medium [J]. Journal of Central South University, 2019, 26(10): 2785−2796. DOI: https://doi.org/10.1007/s11771-019-4213-5.

1 Introduction

The problem of pipes conveying fluid has been a hot issue among scholars all over the world for nearly half-century. In 1993, PAIDOUSSIS et al [1] quoted more than 200 references to systematically illustrated the vibration characteristics, stability and nonlinear dynamics of pipes conveying fluid. They pointed out that the model of pipe conveying fluid had become a new paradigm to investigate dynamical behavior [1]. In the past ten years, the rapid development of micro and nano mechanics has led to the microscale and nanoscale pipes conveying fluid playing a very significant role in many fields, which aroused the scholars' enthusiasm for studying the micro and nano scale pipes conveying fluid.

With the development of microelectronics, micromechanics and biological engineering technology, microfluidic technology has played an indispensable role in the fields of biomedicine, aerospace, chemistry and so on [2−4]. In order to fulfill the special application in engineering, the performance of microfluid carrier is becoming more and more diverse and complicated. FGMs, a new type of composite materials, exhibit a gradient change in their spatial composition, and their corresponding thermodynamic and physical properties also vary in gradient. Compared with

Received date: 2018-06-04; **Accepted date:** 2019-03-12
Corresponding author: LIU Yong-shou, PhD, Professor; Tel: +86-13359234099; E-mail: yongshouliu@nwpu.edu.cn; ORCID: 0000-0002-4205-3026

traditional materials, FGMs have many unique advantages (thermal stress relaxation, graded properties, strong designability), no obvious interface, etc), which can meet the special needs of the engineering materials, so that FGMs are widely used in aerospace, bioengineering, mechanical engineering and other fields [5]. Therefore, researching the dynamic performances of micro-scale FGMs fluid-conveying pipes is very important to practical applications in engineering.

Micro-scale functionally graded fluid-conveying pipes are pipes with diameter from a few microns to hundreds of microns and the properties of the materials gradually vary with the radial or axial. Micron scale materials have micro-scale effect [6−9], so that their properties are different from those of macroscopic materials. DENG et al [10] used a hybrid method to analyze the vibration of multi-span FGM fluid-conveying micropipes. The micro-scale pipe's non-classical Timoshenko beam model was presented by XIA et al [11] and they found that the Poisson effect has a great influence on the vibration characteristics of micro-scale tubes. LIANG et al [12] investigated the thermal elastic vibration of micro-scale conveying fluid pipes in elastic medium. NOROUZZADEH et al [13, 14] analyzed the isogeometric vibration and buckling behavior of functionally graded nanoplates with the consideration of nonlocal and surface effects. CHEN et al [15] studied the dynamic behavior of axially functionally graded pipes conveying fluid.

Although it is not uncommon to research the thermoelastic vibration of pipes, the results obtained by scholars were mostly concentrated on the linear or nonlinear macro-pipes [16−19] and nano-tubes [20−25] yet, micro-pipes received scant attention [26]. The research of the micro-scale pipes conveying fluid is not perfect, especially under the condition that the micro-scale functionally graded material fluid-conveying pipes embedded in elastic medium and considering thermal working environment. In this work, differential quadrature method (DQM) is used to research: the scale effect of microtubule and micro-fluid on dimensionless natural frequency and critical velocity of the micro-scale FGM pipes; the effect of material property index n on dimensionless natural frequency and critical velocity; the effect of elastic coefficient of the elastic matrix on natural frequency of the FGM pipes; the effect of the pipes' external radius on natural frequency of the FGM pipes. These particular features of micro-scale FGM pipes investigated in this paper have some significance for the special applications in engineering.

2 Vibration analysis model and vibration governing equation

The model of micro-scale fluid-conveying pipe embedded in elastic medium is shown in Figure 1. In Figure 1, the length of the pipe is L, the velocity is U, the inner radius is R_i, the outer radius is R_o, and r is the radius of the reference point.

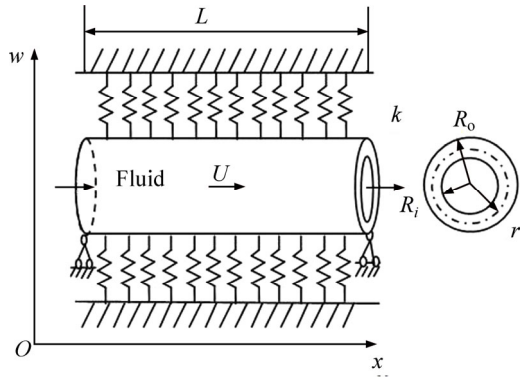

Figure 1 Thermoelastic vibration analysis model of micro-scale FGM fluid-conveying pipe in elastic medium

The properties of the FGM pipe vary continuously along the radials direction, which can be represented as follows [27]:
the elasticity modulus:

$$E(r)=V_{\mathrm{i}}E_{\mathrm{i}}+V_{\mathrm{o}}E_{\mathrm{o}} \tag{1}$$

the shear modulus:

$$G(r)=V_{\mathrm{i}}G_{\mathrm{i}}+V_{\mathrm{o}}G_{\mathrm{o}} \tag{2}$$

pipe density:

$$\rho(r)=V_{\mathrm{i}}\rho_{\mathrm{i}}+V_{\mathrm{o}}\rho_{\mathrm{o}} \tag{3}$$

thermal expansion rate:

$$a(r)=V_{\mathrm{i}}a_{\mathrm{i}}+V_{\mathrm{o}}a_{\mathrm{o}} \tag{4}$$

volume fractions:

$$V_{\mathrm{i}}=\left(\frac{R_{\mathrm{o}}-r}{R_{\mathrm{o}}-R_{\mathrm{i}}}\right)^{n} \tag{5}$$

$$V_{\mathrm{o}}=1-V_{\mathrm{i}} \tag{6}$$

where Poisson ratio v is assumed to be a constant.

V_o is the volume fraction of the outer wall material of the FGM pipe; V_i is the volume fraction of the inner wall material of the pipe; and n is the exponent of the volume fraction. The material properties of different n varying with radius are shown in Figure 2. In Figure 2, P_o is the external material properties and P_i represents internal material properties. The conclusion shows that the larger the pipe has volume fraction, the faster the velocity of the material properties varys from inner to outer.

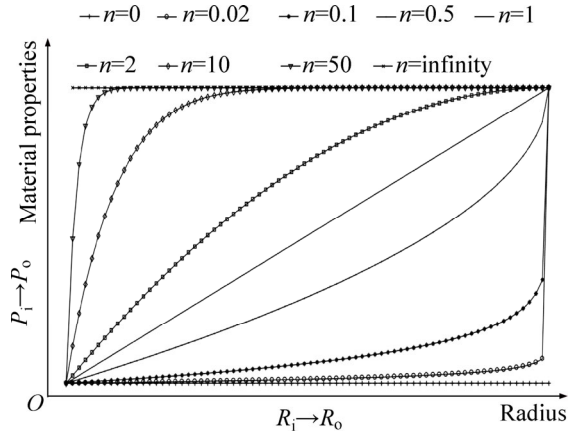

Figure 2 Material properties of different n varying with radius

Classical mechanical theory is no longer applicable at the micron scale. In order to study the size effect of structure, the strain gradient theory and the couple stress theory, as special forms of nonlocal theory, are introduced into the study of micrometer-scale mechanics. Couple stress theory can be regarded as a special form of second order strain gradient theory. In 2002, YANG et al [28] modified the couple stress theory. Since then, many scholars adopted the modified couple stress theory in the studies of microbeam, microplate and microtubule.

According to the modified couple stress theory presented by YANG et al [28], the strain energy of the structures is a function of both strain tensor (conjugated with stress tensor) and curvature tensor (conjugated with couple stress tensor). According to YANG's [28] and Reddy's model [29], the strain energy U can be written as:

$$U_m = \frac{1}{2}\int_{\Omega}(\sigma_{ij}\varepsilon_{ij} + m_{ij}\chi_{ij})\mathrm{d}v \ (i, j = x, y, z) \tag{7}$$

where Ω is the volume,

$$\sigma_{ij} = \lambda tr(\varepsilon_{ij})\delta_{ij} + 2G\varepsilon_{ij} \tag{8}$$

$$\varepsilon_{ij} = \frac{1}{2}[\nabla u_i + (\nabla u_i)^{\mathrm{T}}] \tag{9}$$

$$m_{ij} = 2l^2 G\chi_{ij} \tag{10}$$

$$\chi_{ij} = \frac{1}{2}[\nabla\theta_i + (\nabla\theta_i)^{\mathrm{T}}] \tag{11}$$

Eqs. (8)−(11) represent the stress, the strain tensor, the deviatoric part of the couple stress tensor and the symmetric curvature tensor of the system, respectively. Among them, λ and G are the Lame's constants, u_i is the displacement, δ_{ij} is Kronecker's delta function, l is the parameter of tube micro-scale effect and θ_i is the rotation vector that can be written as

$$\theta_i = \frac{1}{2}cul(u_i) \tag{12}$$

According to the Euler-Bernoulli beam theory, the displacement of the x-, y- and z-axes can be shown as

$$u = -z\psi(x,\ t),\ v = 0,\ w = w(x,\ t) \tag{13}$$

where $\psi(x)$ is the rotation of pipe cross section and by small deformation assumption, it can be shown as

$$\psi(x) \approx \frac{\partial w(x,t)}{\partial x} \tag{14}$$

Substituting Eqs. (13) and (14) into Eq. (9) yields

$$\varepsilon_{xx} = -z\frac{\partial^2 w(x,t)}{\partial x^2},\ \varepsilon_{yy} = \varepsilon_{zz} = \varepsilon_{xy} = \varepsilon_{yx} = \varepsilon_{zx} = 0 \tag{15}$$

Substituting Eqs. (13) and (14) into Eq. (12) yields

$$\theta_y = -\frac{\partial w(x,t)}{\partial x},\ \theta_x = \theta_z = 0 \tag{16}$$

Substituting Eq. (16) into Eq. (11) yields

$$\chi_{xy} = -\frac{1}{2}\frac{\mathrm{d}^2 w(x)}{\mathrm{d}x^2},\ \chi_{xx} = \chi_{yy} = \chi_{zz} = \chi_{yz} = \chi_{zx} = 0 \tag{17}$$

Substituting Eq. (15) into Eq. (8) gives

$$\sigma_{xx} = -Ez\frac{\partial^2 w(x,t)}{\partial x^2},\ \sigma_{yy} = \sigma_{zz} = \sigma_{xy} = \sigma_{yz} = \sigma_{zx} = 0 \tag{18}$$

where E is the elasticity modulus of the FGM micro-scale tube, and the Poisson effect is neglected[30, 31].

Substituting Eq. (18) into Eq. (10) obtains

$$m_{xy} = -Gl^2\frac{\mathrm{d}^2 w(x)}{\mathrm{d}x^2},\ m_{xx} = m_{yy} = m_{zz} = m_{yz} = m_{zx} = 0 \tag{19}$$

Substituting Eqs. (15), (17), (18) and (19) into Eq. (7) can obtain the strain energy of the FGM micro-scale tube.

$$U_m = \frac{1}{2}\int_0^L (EI_{\text{eq}} + GA_{\text{eq}}l^2)\left(\frac{\partial^2 w}{\partial x^2}\right)^2 \mathrm{d}x \tag{20}$$

where

$$\mathrm{EI}_{\text{eq}} = \int_A E(r)z^2 \mathrm{d}A = \int_0^{2\pi}\int_{R_i}^{R_o} E(r)r^2 \sin^2(\theta) r \mathrm{d}r\mathrm{d}\theta \tag{21}$$

and

$$\mathrm{GA}_{\text{eq}} = \int_A G(r)\mathrm{d}A = \int_0^{2\pi}\int_{R_i}^{R_o} G(r) r \mathrm{d}r\mathrm{d}\theta \tag{22}$$

The kinetic energy of the tube can be expressed as

$$T_p = \frac{m}{2}\int_0^L \left(\frac{\partial w}{\partial t}\right)^2 \mathrm{d}x \tag{23}$$

where m is the linear density of the FGM micro-scale fluid-conveying tube that can be shown as

$$m = \int_A \rho(r)\mathrm{d}A = \int_0^{2\pi}\int_{R_i}^{R_o} \rho(r) r \mathrm{d}r\mathrm{d}\theta \tag{24}$$

The kinetic energy of the fluid in the tube can be shown as

$$T_{\text{f}} = \frac{M}{2}\int_0^L \left[\left(\frac{\partial w}{\partial t} + U\frac{\partial w}{\partial x}\right)^2 + U^2\right]\mathrm{d}x \tag{25}$$

where M is the linear density of the fluid in the tube and U is the velocity of the fluid.

Based on the thermoelastic theory, the strain energy caused by temperature variation can be written as

$$U_T = \frac{1}{2}\int_0^L \left[-N_T\left(\frac{\partial w}{\partial t}\right)^2\right]\mathrm{d}x \tag{26}$$

where

$$N_T = -\frac{EAa_{\text{eq}}}{1-2\nu}\Delta T \tag{27}$$

and

$$EAa_{\text{eq}} = \int_A E(r)a(r)\mathrm{d}A = \int_0^{2\pi}\int_{R_i}^{R_o} E(r)a(r) r \mathrm{d}r\mathrm{d}\theta \tag{28}$$

And the potential energy can be kept in elastic medium when the elastic is deforming, which can be written as

$$U_k = \int_0^L (-kw^2)\mathrm{d}x \tag{29}$$

where k is the elastic coefficient of the elastic medium.

According to PAIDOUSSIS [32], the Hamilton's principle can be shown as

$$\delta\int_{t_1}^{t_2} l_{\text{c}}\mathrm{d}t = 0 \tag{30}$$

where the Lagrangian of the system can be expressed as

$$l_{\text{c}} = -U_m + T_{\text{p}} + T_{\text{f}} + U_T + U_k \tag{31}$$

Substituting Eqs. (20), (23), (25), (26), (27) and (31) into Eq. (30), the thermoelastic vibration control equation of the micro-scale fluid-conveying tube in elastic medium can be obtained.

$$(EI_{\text{eq}} + GA_{\text{eq}}l^2)\frac{\partial^4 w}{\partial x^4} + (MU^2 - N_T)\frac{\partial^2 w}{\partial x^2} + 2MU\frac{\partial^2 w}{\partial x\partial t} + (M+m)\frac{\partial^2 w}{\partial t^2} + kw = 0 \tag{32}$$

Considering the influence of the elastic medium, the thermoelastic vibration equation of micro-scale fluid-conveying tubes in elastic medium can be obtained as

$$(EI_{\text{eq}} + GA_{\text{eq}}l^2)\frac{\partial^4 w}{\partial x^4} + (\alpha MU^2 - N_T)\frac{\partial^2 w}{\partial x^2} + 2MU\frac{\partial^2 w}{\partial x\partial t} + (M+m)\frac{\partial^2 w}{\partial t^2} + kw = 0 \tag{33}$$

where α is the parameter of micro-fluid effect [33−35].

The boundary conditions with both ends simply supported can be shown as

$$w(0,\ t) = w(L,\ t) = 0,\ \frac{\partial^2 w(0,t)}{\partial x^2} = \frac{\partial^2 w(L,t)}{\partial x^2} = 0 \tag{34}$$

Dimensionless parameters are introduced as follows:

$$Y = \frac{w}{L}, X = \frac{x}{L},\ \tau' = \left(\frac{EI_{\text{eq}}}{M+m}\right)^{\frac{1}{2}}\frac{t}{L^2},\ \overline{N}_T = \frac{N_T L^2}{EI_{\text{eq}}},$$
$$K = \frac{kL^4}{EI_{\text{eq}}},\ u = \left(\frac{M}{EI_{\text{eq}}}\right)^{\frac{1}{2}} LU,\ \beta = \frac{M}{M+m},\ g = \frac{GA_{\text{eq}}l^2}{EI_{\text{eq}}} \tag{35}$$

Substituting dimensionless parameters in Eq. (35) into the governing Eq. (33) and the boundary conditions (34), the dimensionless equations and dimensionless boundary conditions can be obtained as follows:

$$(1+g)\frac{\partial^4 Y}{\partial X^4}+(\alpha u^2-\overline{N}_T)\frac{\partial^2 Y}{\partial X^2}+2u\sqrt{\beta}\frac{\partial^2 Y}{\partial \tau' \partial X}+\frac{\partial^2 Y}{\partial \tau'^2}+KY=0 \tag{36}$$

$$Y(0,\tau')=Y(1,\tau')=0,\ \frac{\partial^2 Y(0,\tau')}{\partial X^2}=\frac{\partial^2 Y(1,\tau')}{\partial X^2}=0 \tag{37}$$

3 Differential quadrature method

In this study, the differential quadrature method is used to solve the governing equation. In the interval of [a, b], the derivative of the one-dimensional continuous differentiable function $f(x)$ can be expressed as [36, 37]

$$L_n\{f(x_i)\}=\sum_{j=1}^{N}C_{ij}^{(n)}f(x_j) \tag{38}$$

where L_n is a linear differential operator; n is the differential order; $C_{ij}^{(n)}$ is the weighting coefficient; x_j is the j coordinate values in N mutually different nodes; a=x_1 and b=x_N are the first and last point, respectively.

The first derivative weighting coefficient is

$$C_{ij}^{(1)}=l_j'(x_i)=\begin{cases}\prod_{k=1,k\neq i,j}^{N}(x_i-x_k)\Big/\prod_{k=1,k\neq j}^{N}(x_j-x_k)\\ \sum_{k=1,k\neq i}^{N}\frac{1}{(x_i-x_k)}\ (i=j)\end{cases}$$
$$i,\ j=1,\ 2,\ \cdots,\ N \tag{39}$$

where $l_j(x)$ is Lagrange interpolation function.

The recurrence formula of weighted coefficients is

$$C_{ij}^{(2)}=\sum_{k=1}^{N}C_{ik}^{(1)}C_{kj}^{(1)},$$
$$C_{ij}^{(3)}=\sum_{k=1}^{N}C_{ik}^{(1)}C_{kj}^{(2)}=\sum_{k=1}^{N}C_{ik}^{(2)}C_{kj}^{(1)},$$
$$C_{ij}^{(4)}=\sum_{k=1}^{N}C_{ik}^{(1)}C_{kj}^{(3)}=\sum_{k=1}^{N}C_{ik}^{(3)}C_{kj}^{(1)} \tag{40}$$

In this study, the Fung node[38] can be expressed as

$$x(i)=\frac{1}{2}\left(1-\cos\frac{i\pi}{N-3}\right),\ i=1,\ 2,\ \cdots,\ N_0\ (N_0=N-4)$$
$$x(N_0+1)=0,\ x(N_0+2)=\frac{1}{2}x(1),$$
$$x(N_0+3)=\frac{1}{2}[x(N_0)+1],\ x(N)=1 \tag{41}$$

Substituting Eq. (38) into Eqs. (36) and (37) obtains

$$\begin{bmatrix}K_{\mathrm{dd}}^1 & K_{\mathrm{db}}^1\\ K_{\mathrm{bd}}^1 & K_{\mathrm{bb}}^1\end{bmatrix}\begin{Bmatrix}\{Y_{\mathrm{d}}\}\\ \{Y_{\mathrm{b}}\}\end{Bmatrix}+\begin{bmatrix}G_{\mathrm{dd}}^1 & G_{\mathrm{db}}^1\\ [0] & [0]\end{bmatrix}\begin{Bmatrix}\{\dot{Y}_{\mathrm{d}}\}\\ \{\dot{Y}_{\mathrm{b}}\}\end{Bmatrix}+\begin{bmatrix}M_{\mathrm{dd}}^1 & M_{\mathrm{db}}^1\\ [0] & [0]\end{bmatrix}\begin{Bmatrix}\{\ddot{Y}_{\mathrm{d}}\}\\ \{\ddot{Y}_{\mathrm{b}}\}\end{Bmatrix}=0 \tag{42}$$

where subscript b and d represent the inner and outer points of the interval; "." means differentiation of time. Matrix K_{dd}^1, K_{db}^1, K_{bd}^1, K_{bb}^1, G_{dd}^1, G_{db}^1, M_{dd}^1, M_{db}^1 can be expressed as

$$K_{\mathrm{dd}}^1=(1+g)\left[C_{ij}^{(4)}\right]_{N_0\times N_0}+(\alpha u^2-\overline{N}_T)\left[C_{ij}^{(2)}\right]_{N_0\times N_0}+K[I]_{N_0\times N_0},$$
$$K_{\mathrm{db}}^1=(1+g)\left[C_{ij}^{(4)}\right]_{N_0\times N_0+1:N}+(\alpha u^2-\overline{N}_T)\left[C_{ij}^{(2)}\right]_{N_0\times N_0+1:N},$$
$$K_{\mathrm{bd}}^1=\left[\{0\}\quad C_{N_0+2,j}^{(2)}\quad C_{N_0+3,j}^{(2)}\quad \{0\}\right]^{\mathrm{T}},\ j=1,\ 2,\ \cdots,\ N_0,$$
$$K_{\mathrm{bb}}^1=\begin{bmatrix}1 & 0 & 0 & 0\\ C_{N_0+2,N_0+1:N}^{(2)} & & & \\ C_{N_0+3,N_0+1:N}^{(2)} & & & \\ 0 & 0 & 0 & 1\end{bmatrix},$$
$$G_{\mathrm{dd}}^1=2u\sqrt{\beta}\left[C_{ij}^{(1)}\right]_{N_0\times N_0},$$
$$G_{\mathrm{db}}^1=2u\sqrt{\beta}\left[C_{ij}^{(1)}\right]_{N_0\times N_0+1:N},$$
$$M_{\mathrm{dd}}^1=[I]_{N_0\times N_0},\ M_{\mathrm{db}}^1=[0]_{N_0\times N_0+1:N} \tag{43}$$

The solution of Eq. (42) can be written as

$$\{Y\}=\{\overline{Y}\}\exp(\omega\tau') \tag{44}$$

where $\{\overline{Y}\}=\{\{\overline{Y_d}\}^{\mathrm{T}}\ (\{\overline{Y_d}\}^{\mathrm{T}}\}^{\mathrm{T}}$ is the amplitude of the micro-scale FGM pipes), Im(ω) is the natural frequency.

Substituting Eq. (44) into Eq. (42) a homogeneous equation about the generalized eigenvalue problem can be obtained as

$$(\omega^2[M^1]+\omega[G^1]+[K^1])\{\overline{Y_d}\}=\{0\} \tag{45}$$

where $M^1=M_{\mathrm{dd}}^1-M_{\mathrm{db}}^1K_{\mathrm{bb}}^{1-1}K_{\mathrm{bd}}^1$ is the mass matrix of the system; $G^1=G_{\mathrm{dd}}^1-G_{\mathrm{db}}^1K_{\mathrm{bb}}^{1-1}K_{\mathrm{bd}}^1$ is the damping matrix of the system; $K^1=K_{\mathrm{dd}}^1-K_{\mathrm{db}}^1K_{\mathrm{bb}}^{1-1}K_{\mathrm{bd}}^1$ is the stiffness matrix of the system.

If Eq. (45) has nonzero solutions, Eq. (46) should be satisfied

$$\det(\omega^2[M^1]+\omega[G^1]+[K^1])=0 \tag{46}$$

where ω is the eigenvalue of the system, which is usually a complex number. The real and imaginary parts represent system damping and vibration frequency, respectively.

Set

$$B=\begin{bmatrix}-[M^1]^{-1}[G^1] & -[M^1]^{-1}[K^1]\\ [I] & [0]\end{bmatrix} \tag{47}$$

then, the two-dimensional eigenvalue problem can be simplified as

$$\det(B-\omega I)=0 \tag{48}$$

4 Results and discussion

The FGM micro-scale pipe researched in this study is composed of metal Ti−6Al−4V and ceramic ZrO_2 [39]. The material properties are changed from outer ceramic material to the inner metal material. The material properties of the FGM pipe are chosen to be E_i=116.7 GPa, E_o=151.0 GPa, ρ_i=4420 kg/m^3, ρ_o=5331 kg/m^3, v=1/3, $G_i=E_i/2(1+v)$, $G_o=E_o/2(1+v)$, $a_i=9.5\times10^{-6}$ K^{-1}, $a_o=10.0\times10^{-6}$ K^{-1}, R_i=7.5 μm, R_o=15 μm, $L/(2R_o)$=100 (the ratio of length to diameter). The micro-scale FGM pipe characteristics of size can be expressed as $l=b_h/[3(1-v)]$ where b_h=24 μm, and l=17 μm can be obtained [8, 40]. The micro scale parameter of the fluid takes α=4/3.

In order to verify the solving method used in this paper, the result is compared with the results of WANG [40]. Figure 3 shows that in the same situation (E=1.44 GPa, $\rho_f=\rho_p$=1000 kg/m^3, μ=0.38, l=17.6, d/D=0.8, L/D=20, D=50 μm) the relationship between natural frequency and flow velocity calculated by the program in this study is consistent with the reference.

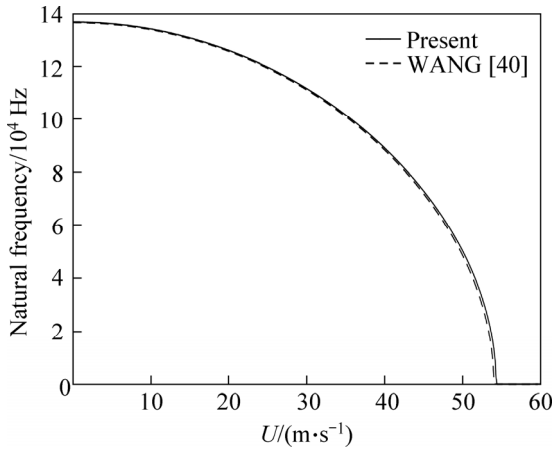

Figure 3 Relationship between natural frequency and flow velocity

The effect of the microscale effect and micro-fluid effect on the natural frequency and critical velocity of the micro-scale FGM pipe is shown in Figure 4. In Figure 4, let K=10^6 kPa, n=1, ΔT=0, 10, 20, 30 K. In Figure 4(a), let l=0, a=1. In Figure 4(b), take l=17 μm, a=1. In Figure 4(c), choose l=17 μm, a=4/3.

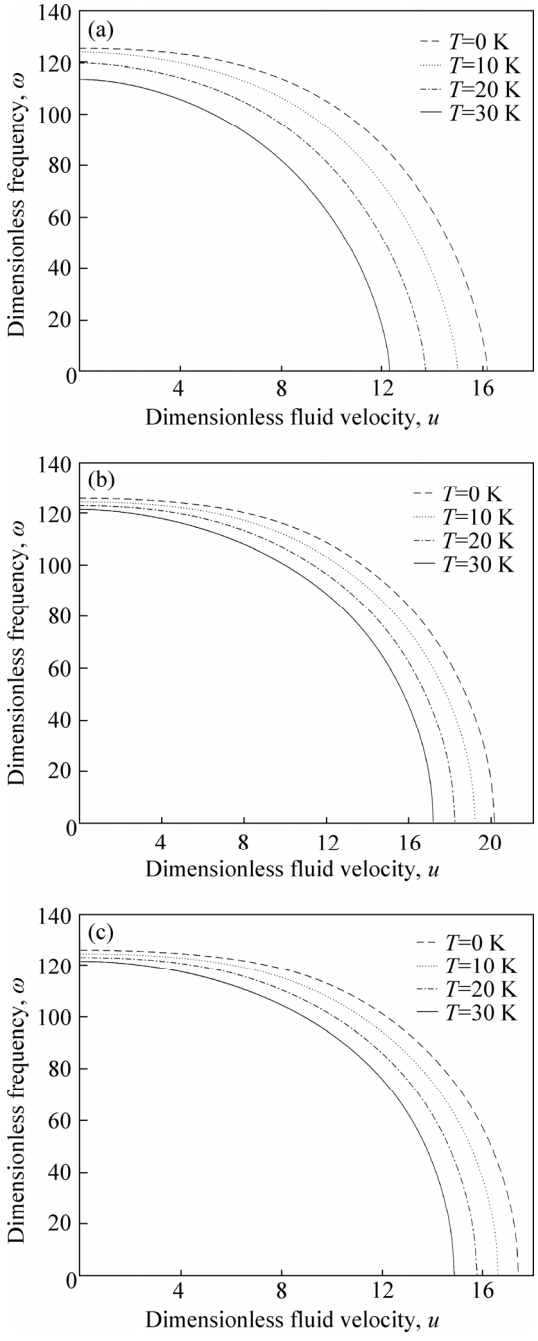

Figure 4 Effect of microscale effect and micro-fluid effect on natural frequency and critical velocity of micro-scale FGM pipe: (a) l=0, a=1; (b) l=17 μm, a=1; (c) l=17 μm, a=4/3

Figure 4 shows that with the increase of temperature, both of the first-order dimensionless natural frequency and the critical dimensionless velocity decrease. On the other hand, it can be found from Figure 4 that with the increase of dimensionless velocity, the first-order dimensionless natural frequency gradually decreased to 0. The eigenvalue of the system in this paper is a function of the liquid velocity. With the increase of velocity, the stiffness of the system decreases and the system stiffness disappears when the velocity reaches a certain value (the vibrational frequency of the system is 0). When the first-order dimensionless vibration frequency arrives 0, the system enters an unstable state (static buckling instability), and the corresponding dimensionless velocity is the critical dimensionless velocity of the FGM pipe.

In order to research the effect of the microscale effect and micro-fluid effect on the natural frequency and critical velocity of the micro-scale FGM pipe, Figures 4(a) and (b) are compared first. Figure 4 exhibits that the dimensionless critical velocity of the pipe considering the effect of the microscale effect (l=17 μm, a=1) is significantly larger than the dimensionless critical velocity of the classical FGM pipe (l=0, a=1). In other words, the microscale effect will significantly increase the stability of the system. Figures (b) and (c) show that the dimensionless critical flow velocity of the FGM pipe considering the effect of the microscale effect (l=17 μm, a=1) is larger than the critical velocity of the FGM pipe considering the effect of the microscale effect and micro-fluid effect (l=17 μm, a=4/3). In other words, the micro-fluid effect will reduce the stability of the system. Figures 4(a) and (c) show that the dimensionless critical velocity of the microscale FGM pipe (l=17 μm, a=4/3) is greater than the dimensionless critical velocity of the classical FGM pipe (l=0, a=1). The calculation according to the classical model will seriously underestimate the stability of the system, which causes a great influence on practical application in engineering.

The effect of the microscale effect and micro-fluid effect on first two natural frequencies of the micro-scale FGM pipe is shown in Figure 5. In Figure 5, let K=0 Pa, n=1, ΔT=0 K. In Figures 5(a) and (b), let l=17 μm, a=4/3. In Figures 5(c) and (d) take (l=0, a=1). The stability of the FGM pipe can be divided into three situations: stable state (Im(ω)>0 and Re (ω)=0); static instability (Im(ω)=0 and Re (ω) have negative value); dynamic instability (Im(ω)>0 and Re (ω) have negative value).

Figures 5(a) and (b) shows that the 1st-mode static instability occurs at u=4.466 (1st-mode critical velocity), the 2nd-mode static instability occurs at u=8.932 (2nd-mode critical velocity). When the fluid velocity increases to 9.23, the first order natural frequency and the second order natural frequency overlap, which leads to the coupling dynamic instability in the first and second order modes. Figures 5(c) and (d) shows that the 1st-mode static instability occurs at u=3.205, the 2nd-mode static instability occurs at u=6.392. When the fluid velocity increases to 6.55, the first order natural frequency and the second order natural frequency overlap, which leads to the coupling dynamic instability in the first and second order modes. According to the result, we can conclude that the FGM pipe considering the effect of the microscale effect and micro-fluid effect has higher 1st-mode critical velocity and 2nd-mode critical velocity (the stability of the system is higher), but the instability pattern has not changed.

The effect of the exponent n of material property on the natural frequency and critical velocity of the micro-scale FGM pipe is shown in Figure 6. In the figure, take K=10^6 Pa, ΔT=10 K, n=0, 0.1, 0.5, 1, 2, 10.

Figure 6 shows that when the dimensionless velocity is 0, the smaller the n is, the higher the dimensionless natural frequency is. With the increase of dimensionless velocity, the dimensionless natural frequency of system decreases. The smaller the n is, the bigger the rate of descent is. When the velocity reaches the critical dimensionless velocity. The bigger the n is, the greater the dimensionless critical velocity is. In other words, with the increase of n, the volume fraction of the external material increases gradually, and the decrease rate of the dimensionless natural frequency decreases gradually, but the dimensionless critical velocity increases with it.

The effect of the elastic coefficient of the elastic medium on the natural frequency of the micro-scale FGM pipe is shown in Figure 7. In Figure 7(a), let U=1 m/s, n=1, ΔT=0 K, 10 K, 20 K, 30 K. In Figure 7(b), let U=1 m/s, ΔT=10 K, n=0,

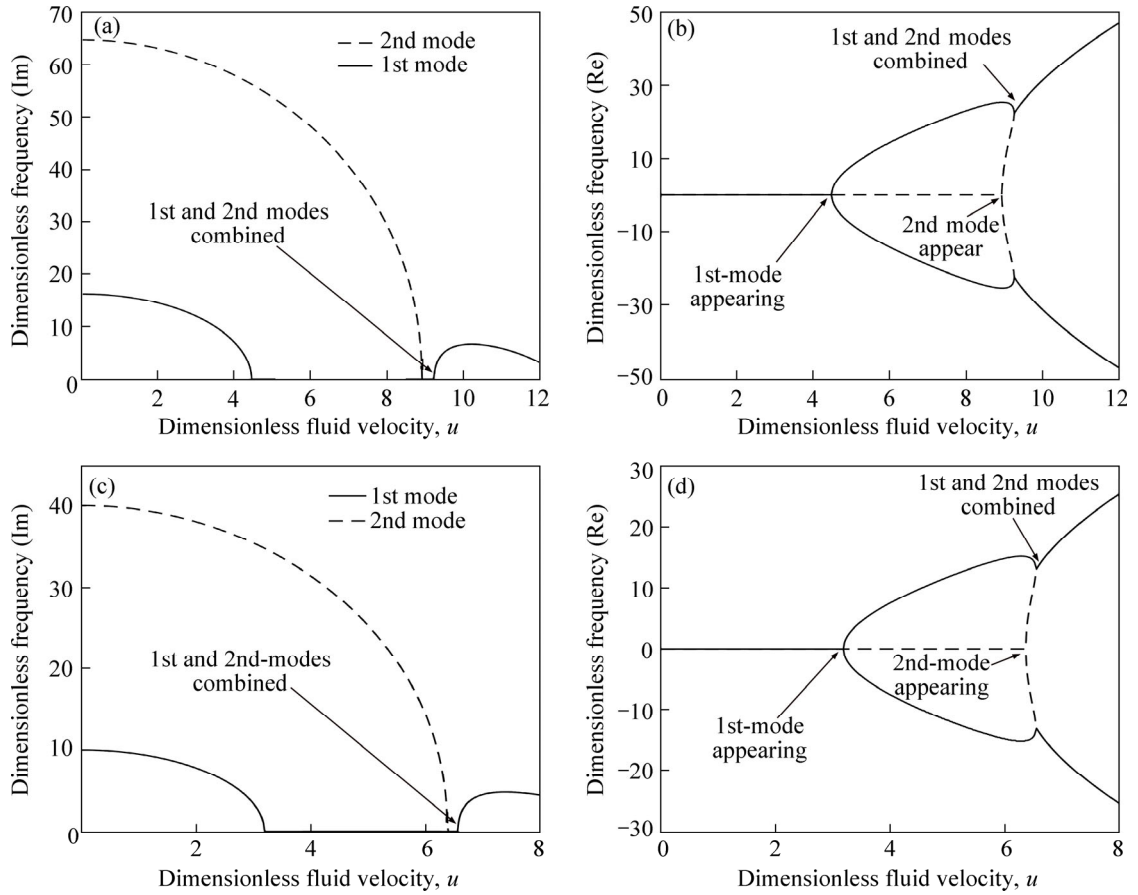

Figure 5 Effect of microscale effect and micro-fluid effect on first two natural frequencies of micro-scale FGM pipe: (a, b) l=17 μm, a=4/3; (c, d) l=0, a=1

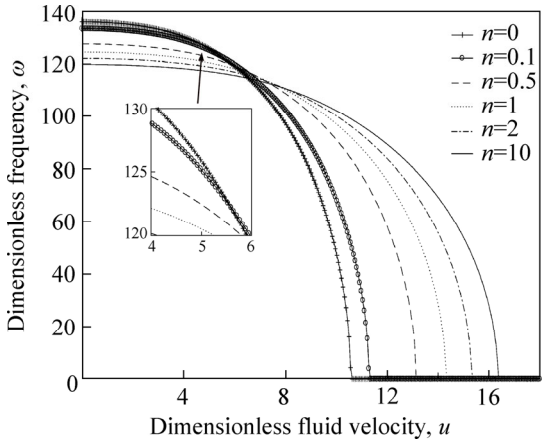

Figure 6 Effect of exponent n of material property on natural frequency and critical velocity of micro-scale FGM pipe

0.1, 0.5, 1, 2, 10.

It can be seen from Figure 7 that the dimensionless vibration frequency of the system increases with the increase of the elastic coefficient K, and its increase trend has no significant change. In other words, the influence of K on dimensionless vibration frequency is almost linear in a certain range.

The effect of the material property exponent change on the natural frequency of the micro-scale FGM pipe is shown in Figure 7. In the figure, let U=1 m/s, K=10^6 Pa, ΔT=0, 10, 20, 30 K.

It can be seen from Figure 8 that the dimensionless vibration frequency of the system decreases with the increase of the exponent n, and the dimensionless vibration frequency decreases more slowly with the increasing of n. In other words, with the increase of n, the volume fraction of outer material increases. The increases of the volume fraction of outer material lead to the decrease of the dimensionless frequency of the system. When n increases to a certain extent, the rate of the volume fraction change becomes slow that makes the dimensionless natural frequencies drop more slowly.

The effect of the outer radius change on the natural frequency of the micro-scale FGM pipe is shown in Figure 9. In Figure 9(a), let U=1 m/s, K=10^6 Pa, ΔT=0, 10, 20, 30 K, n=1. In Figure 9(b),

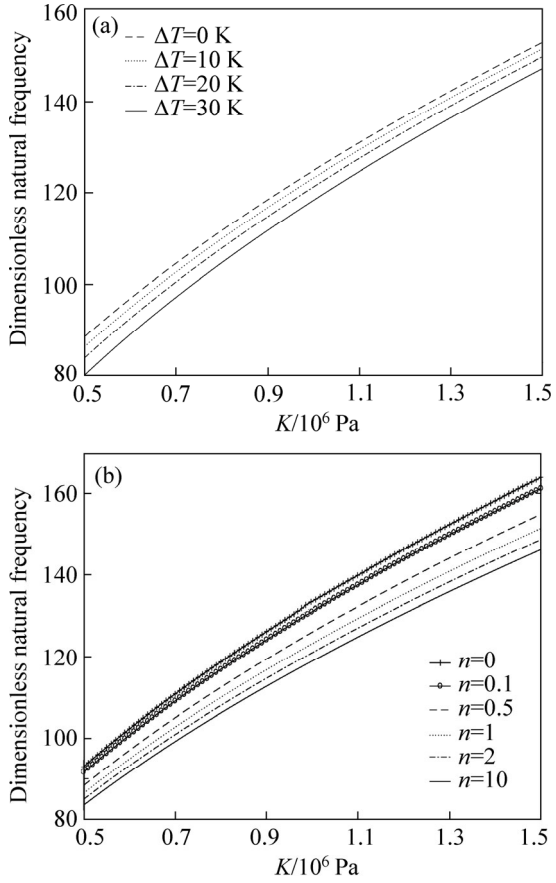

Figure 7 Elastic coefficient of elastic medium on natural frequency of micro-scale FGM pipe

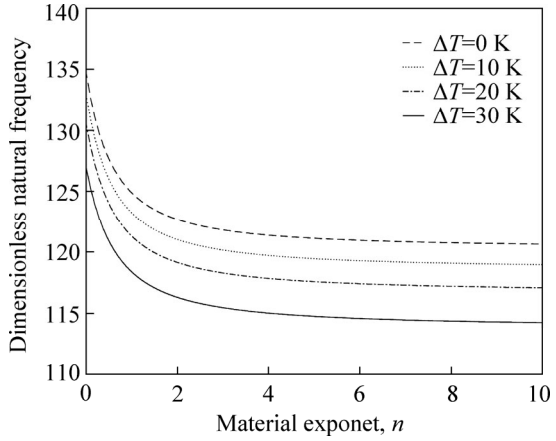

Figure 8 Effect of material property exponent change on natural frequency of micro-scale FGM pipe (different exponent n)

let U=1 m/s, K=10^6 Pa, ΔT=10 K, n=0, 0.1, 0.5, 1, 2, 10.

It can be seen from Figure 9 that the dimensionless vibration frequency decreases with the increase of the external radius, and the rate of decline becomes slower with the increase of the external radius. In other words, with the increase of

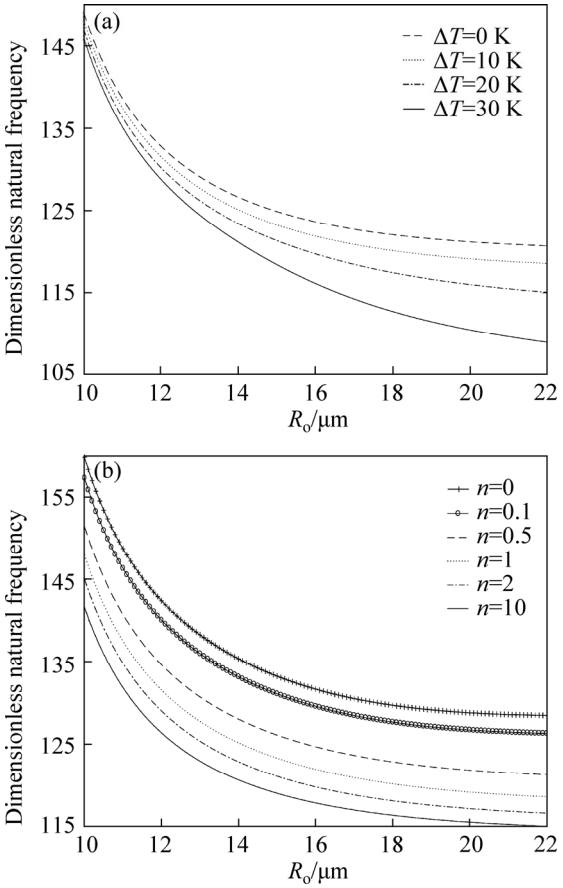

Figure 9 Effect of outer radius change on natural frequency of micro-scale FGM pipe: (a) Different temperature; (b) Different exponent n

the external radius, the effect of the outer radius change on the natural frequency of the micro-scale FGM pipe is gradually reduced.

The effect of the different boundary conditions on the natural frequency and critical velocity of the micro-scale FGM pipe is shown in Figure 10. In

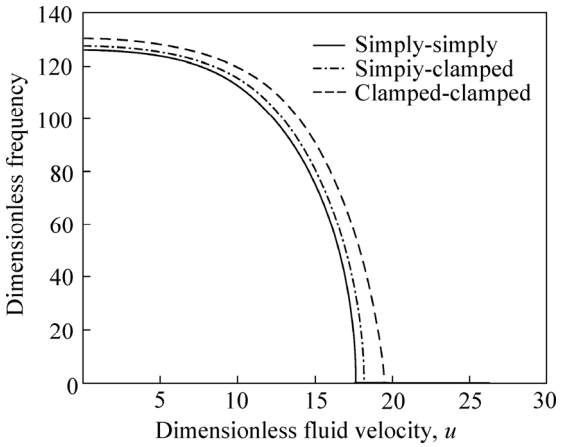

Figure 10 Effect of different boundary conditions on natural frequency and critical velocity of micro-scale FGM pipe

Figure 10, let $K=10^6$ Pa, $n=1$, $\Delta T=0$ K. Figure 9 shows that the micro-scale FGM pipe with the boundary conditions of clamped-clamped has the highest critical velocity and it also has the highest natural frequency at the same fluid velocity. The stability of the micro-scale FGM pipe with the boundary conditions of simply-clamped is higher than the micro-scale FGM pipe with the boundary conditions of simply-simply.

5 Conclusions

In this work, the differential equation of micro-scale functionally graded fluid-conveying pipes in elastic medium is established by considering various factors comprehensively. Some main conclusions are shown as follows:

1) With the increase of the temperature, the dimensionless natural frequency and the dimensionless critical velocity of the system will decrease, and the stability of the system will decrease.

2) The scale effect of the micropipe can improve the dimensionless critical velocity of the system (improve the stability of the system). The micro-fluid effect can reduce the dimensionless critical velocity of the FGM pipe (decrease the stability of the system). Under the condition of considering, the scale effect and micro-fluid effect, the dimensionless critical velocity of the FGM pipe is higher than the dimensionless critical velocity of the classical macroscopic model. In other words, the effect of the scale effect and the micro-fluid effect improve the stability of the system greatly. With the fluid velocity increases, when the fluid velocity reaches a certain value, the pipe enters the first order static instability state, the fluid velocity continues to increase and the pipe enters the second order static instability state, and finally the FGM pipe enters the coupled dynamic instability state under the first mode and the second mode.

3) The dimensionless vibration frequency of the system rises with the increase of elastic coefficient K.

4) With the increase of the exponent n, the volume fraction of the external material increases gradually and the dimensionless natural frequency of the system decreases. When n increases to a certain value, the volume fraction will change slowly, which leads to the dimensionless natural frequency decrease more slowly.

5) The dimensionless vibration frequency decreases with the increase of the external radius. With the increase of the external radius the effect of the outer radius change on the natural frequency of the micro-scale FGM pipe is gradually reduced (the rate of descent of the radius changes from 1×10^{-5} m to 1.2×10^{-5} m; about 15 times the rate of descent of the radius changes from 2×10^{-5} m to 2.2×10^{-5} m).

6) The stability relation of micro-scale FGM pipe with different boundary conditions is clamped-clamped>simply-clamped>simply-simply.

References

[1] PAIDOUSSIS M P, LI G X. Pipes conveying fluid: A model dynamical problem [J]. Journal of Fluids and Structures, 1993, 7(2): 137−204.

[2] CAGGIONI M, TRAINI D, YOUNG P M, SPICER P T. Microfluidic production of endoskeleton droplets with controlled size and shape [J]. Powder Technology, 2018, 329: 129−136.

[3] VALENCIA P M, FAROKHZAD O C, KARNIK R, LANGER R. Microfluidic technologies for accelerating the clinical translation of nanoparticles [J]. Nature Nanotechnology, 2012, 7(10): 623−629.

[4] ELVIRA K S, CASADEVALL X C I, WOOTTON R C R, DEMELLO A J. The past, present and potential for microfluidic reactor technology in chemical synthesis [J]. Nature Chemistry, 2013, 5(11): 905−915.

[5] YANG Hai-lin, LI Jing, FANG Hua-chan, ZHOU Zhong-cheng, TONG Xiao-yang, RUAN Jian-ming. Synthesis, characterization and biological activity in vitro of FeCrAl(f)/HA asymmetrical biological functionally gradient materials [J]. Journal of Central South University, 2014, 21(2): 447−453.

[6] MA Q, CLARKE D R. Size dependent hardness of silver single crystals [J]. Journal of Materials Research, 1995, 10(4): 853−863.

[7] CHONG A C M, LAM D C C. Strain gradient plasticity effect in indentation hardness of polymers [J]. Journal of Materials Research, 1999, 14(10): 4103−4110.

[8] LAM D C C, YANG F, CHONG A C M, WANG J, TONG P. Experiments and theory in strain gradient elasticity [J]. Journal of the Mechanics and Physics of Solids, 2003, 51(8): 1477−1508.

[9] MCFARLAND A W, COLTON J S. Role of material micro-structure in plate stiffness with relevance to microcantilever sensors [J]. Journal of Micromechanics and Microengineering, 2005, 15(5): 1060−1067.

[10] DENG J, LIU Y, LIU W. Size dependent vibration analysis of multi span functionally graded material micropipes conveying fluid using a hybrid method [J]. Microfluidics and Nanofluidics, 2017, 21(8): 1−15.

[11] XIA W, WANG L. Microfluid-induced vibration and stability of structures modelled as microscale pipes conveying fluid

based on non-classical Timoshenko beam theory [J]. Microfluidics and Nanofluidics, 2010, 9(4, 5): 955−962.

[12] LIANG F, BAO R. Thermoelastic vibration of fluid-conveying microtubes embedded in elastic mediume [J]. Mechanics in Engineering, 2014, 36(6): 728−732.

[13] NOROUZZADEH A, ANSARI R. Isogeometric vibration analysis of functionally graded nanoplates with the consideration of nonlocal and surface effects [J]. Thin-Walled Structures, 2018, 127: 354−372.

[14] ANSARI R, NOROUZZADEH A. Nonlocal and surface effects on the buckling behavior of functionally graded nanoplates: An isogeometric analysis [J]. Physica E: Low-dimensional Systems and Nanostructures, 2016, 84: 84−97.

[15] CHEN A, JIAN S. Dynamic behavior of axially functionally graded pipes conveying fluid [J]. Mathematical Problems in Engineering, 2017, 2017(1): 1−11.

[16] SHENG G G, WANG X. Dynamic characteristics of fluid-conveying functionally graded cylindrical shells under mechanical and thermal loads [J]. Composite Structures, 2011, 93(1): 162−170

[17] SOFIYEV A H, HUI D, HUI V C, ERDEM H, YUAN G Q, SCHNACK E, GULDAL V. The nonlinear vibration of orthotropic functionally graded cylindrical shells surrounded by an elastic foundation within first order shear deformation theory [J]. Composites Part B: Engineering, 2017, 116: 170−185.

[18] ZHANG Z, LIU Y, HAN T. Two parameters affecting the dynamics characteristics of a uniform conical assembled pipe conveying fluid [J]. Journal of Vibration and Control, 2017, 23(3): 361−372.

[19] LI B, GAO H, LIU Y, YUE Z. Transient response analysis of multi span pipe conveying fluid [J]. Journal of Vibration and Control, 2013, 19(14): 2164−2176.

[20] ANSARI R, GHOLAMI R, NOROUZZADEH A. Size-dependent thermo-mechanical vibration and instability of conveying fluid functionally graded nanoshells based on Mindlin's strain gradient theory [J]. Thin-Walled Structures, 2016, 105: 172−184.

[21] ANSARI R, NOROUZZADEH A, GHOLAMI R, FAGHIH SHOJAEI M, HOSSEINZADEH M. Size-dependent nonlinear vibration and instability of embedded fluid-conveying SWBNNTs in thermal environment [J]. Physica E: Low-dimensional Systems and Nanostructures, 2014, 61: 148−157.

[22] ZHANG Y W, ZHOU L, FANG B, YANG T Z. Quantum effects on thermal vibration of single-walled carbon nanotubes conveying fluid [J]. Acta Mechanica Solida Sinica, 2017, 30(5): 550−556.

[23] ZHEN Y, FANG B. Thermal mechanical and nonlocal elastic vibration of single walled carbon nanotubes conveying fluid [J]. Computational Materials Science, 2010, 49(2): 276−282.

[24] ZHANG Z, LIU Y, ZHAO H, LIU W. Acoustic nanowave absorption through clustered carbon nanotubes conveying fluid [J]. Acta Mechanica Solida Sinica, 2016, 29(3): 257−270.

[25] ZHANG Z, LIU Y, ZHAO H, LIU W. Topology optimized vibration control of a fluid-conveying carbon nanotube with non-uniform magnetic field [J]. International Journal of Applied Mechanics, 2015, 7(6): 1550092.

[26] ANSARI R, GHOLAMI R, NOROUZZADEH A, SAHMANI S. Size-dependent vibration and instability of fluid-conveying functionally graded microshells based on the modified couple stress theory [J]. Microfluidics and Nanofluidics, 2015,19(3): 509−522.

[27] SETOODEH A R, AFRAHIM S. Nonlinear dynamic analysis of FG micro-pipes conveying fluid based on strain gradient theory [J]. Composite Structures, 2014, 116(1): 128−135.

[28] YANG F, CHONG A C M, LAM D C C, TONG P. Couple stress based strain gradient theory for elasticity [J]. International Journal of Solids and Structures, 2002, 39(10): 2731−2743.

[29] REDDY J N. Microstructure-dependent couple stress theories of functionally graded beams [J]. Journal of the Mechanics and Physics of Solids, 2011, 59(11): 2382−2399.

[30] ASGHARI M, AHMADIAN M T, KAHROBAIYAN M H, RAHAEIFARD M. On the size-dependent behavior of functionally graded microbeams [J]. Materials and Design, 2010, 31(5): 2324−2329.

[31] NATEGHI A, SALAMAT-TALAB M. Thermal effect on size dependent behavior of functionally graded microbeams based on modified couple stress theory [J]. Composite Structures, 2013, 96: 97−110.

[32] PAIDOUSSIS M P. Fluid-structure interaction: Slender structures and axial flow [M]. New York: Academic Press, 2014.

[33] WANG L, LIU H T, NI Q, WU Y. Flexural vibrations of microscale pipes conveying fluid by considering the size effects of micro-flow and micro-structure [J]. International Journal of Engineering Science, 2013, 71(71): 92−101.

[34] GUO C Q, ZHANG C H, PAIDOUSSIS M P. Modification of equation of motion of fluid-conveying pipe for laminar and turbulent flow profiles [J]. Journal of Fluids and Structures, 2010, 26(5): 793−803.

[35] KUTIN J, BAJSIC I. Fluid-dynamic loading of pipes conveying fluid with a laminar mean-flow velocity profile [J]. Journal of Fluids and Structures, 2014, 50: 171−183.

[36] WANG Yong-liang. Differential quadrature method and differential quadrature element method—Theory and application [D]. Nanjing: Nanjing University of Aeronautics and Astronautics, 2001. (in Chinese)

[37] ZHEN Ya-xin. Investigation on the dynamical behavior of carbon nanotubes conveying fluid [D]. Harbin: Harbin Institute of Technology, 2012. (in Chinese)

[38] FUNG T C. Imposition of boundary conditions by modifying the weighting coefficient matrices in the differential quadrature method [J]. International Journal of Numerical Mathematic Engineering, 2003, 56(3): 405−432.

[39] XU Yang-jian, ZHANG Jing-jun, TU Dai-hui. Transient thermal stress analysis of functionally gradient material plate with temperature-dependent material properties under convective heat transfer boundary [J]. Chinese Journal of Mechanical Engineering, 2005, 41(7): 198−204. (in Chinese)

[40] WANG L. Size-dependent vibration characteristics of fluid-conveying microtubes [J]. Journal of Fluids and Structures, 2010, 26(4): 675−684.

(Edited by HE Yun-bin)

中文导读

弹性介质中的微尺度功能梯度材料管热弹性振动分析

摘要：微尺度功能梯度材料输流微管在许多工程领域有着十分重要的应用价值。本文采用修正的偶应力理论和哈密顿原理建立了振动方程，并通过微分求积法求解研究嵌入弹性介质的微尺度功能梯度材料输流管的热弹性振动问题。综合考虑温度变化、微尺寸效应、微流体效应、材料属性变化、弹性基体的弹性系数变化和管道外径变化对微尺度功能梯度材料输流管的热弹性振动影响。研究结果表明：在考虑微尺度和微流体效应的情况下，系统的无量纲临界流速高于经典模型下的系统无量纲临界流速；温度、材料属性、弹性基体的弹性系数、管道外径等因素的变化对系统的一阶固有频率都有显著的影响。

关键词：功能梯度材料；热弹性振动；微尺度；微流体